Article:
Liu, Y, Liu, R orcid.org/0000-0003-0627-3184, Wei, C et al. (2 more authors) (2022) Distributed model predictive control strategy for constrained high-speed virtually coupled train set. IEEE Transactions on Vehicular Technology, 71 (1). pp. 171-183. ISSN 0018-9545

https://doi.org/10.1109/TVT.2021.3130715

Distributed model predictive control strategy for constrained high-speed virtually coupled train set

Yafei Liu, Ronghui Liu, Chongfeng Wei, Jing Xun, and Tao Tang, *Senior Member, IEEE*

***Abstract*—Virtual Coupling (VC) is regarded as a breakthrough to the traditional train operation and control for improving the capability and flexibility in railways. It brings benefits as trains under VC are allowed to operate much closer to one another, forming a virtually coupled train set (VCTS). However, the safe and stable spacing between trains in the VCTS is a problem since there are no rigid couplers to connect them into a fixed formation, especially in high-speed scenarios. Due to the close spacing, the interference between trains becomes non-negligible as various maneuvers of the preceding train can significantly affect driving behaviors of the following train; this results in fluctuating spacing and therefore an unstable VCTS. Aiming at minimizing the interference and maintaining constantly safe spacing between trains in the VCTS, this paper presents a distributed model predictive control (DMPC) approach for solving the high-speed VCTS control problem. Particularly, the proposed control method focuses on the feasibility and stability of this problem, with considerations of the coupled constraint of safety braking distance and the individual constraints of speed limit variations and restricted traction/braking performance. To guarantee feasibility and stability, the terminal controller and invariant set of the DMPC are designed. For rigor, sufficient conditions of feasibility and stability are mathematically proved and derived. Based on the data of the Beijing-Shanghai high-speed railway line, numerical experiments are conducted to verify the correctness of derived sufficient conditions and the effectiveness of the proposed control method under interference and disturbances.**

***Index Terms*—High-speed train, virtual coupling, distributed model predictive control, asymptotic stability**

I. Introduction

HIGH-SPEED railway (HSR) plays a critical role in mass transportation because of the short journey time and convenient travel experience provided for passengers. In recent years, passenger demand for HSR travel in China has had an annual growth rate of more than 10%. In order to meet the growing travel demand in high-speed railways, a constant interest of railway operators is to improve the network capacity by finding a way that could further reduce the spacing between two successive running trains. Through the closer running of trains, there will be ideally zero capacity waste thus improving the train operation with more flexible and versatile service during peak hours [1].

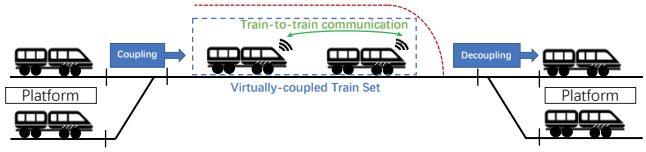

Fig. 1. Illustration of Virtual Coupling concept.

The minimum spacing between trains is directly determined by the separation principle of the Block System within the train control system. The principle states that the spacing between adjacent trains should not be less than the margin value specified by the Block System [2]. Currently, the moving block system (MBS) allows the minimum spacing. Trains under MBS are separated in a sufficient spacing calculated by the absolute braking distance of the train (i.e., the distance that the train is able to reach a standstill from the current speed). Nevertheless, minimum spacing under MBS still cannot meet the demand in high-speed scenarios as the absolute braking distance increases sharply with the raising of the operation speed, e.g., 6.5 km at 350 km/h [3].

Building upon MBS, Virtual Coupling (VC), an emerging technology, is widely recognized as a promising solution to further minimize the spacing between trains. This is achieved by adopting the principle of the relative braking distance (as opposed to the absolute braking distance in MBS), that is, the difference between the braking distances of two successive trains. For the innovative concept of VC to become a reality, two key technical challenges have been identified in the European Shift2Rail Innovation Programmes [4]. First, trains within the virtually coupled train set (VCTS) under VC should be able to operate at a close distance to one another; this is realized by the exchanged state information (e.g., the position, velocity, and acceleration) via train-to-train (T2T) communication. Second, it should be able to dynamically modify the composition of VCTS on the move, involving the operations of coupling and decoupling of trains to and from VCTS. Fig. 1 illustrates the two key properties of the VC concept.

This paper addresses the first technical challenge and focuses more specifically on the stable control problem for the VCTS operating under close spacing. The second challenge

This work was supported by the National Natural Science Foundation of China under Grants 62073026, 7189072 and 7189070, the Fundamental Research Funds for the Central Universities under Grant 2018JBZ006, Beijing Jiaotong University under Grant RCS2021ZT007, and the Royal Academy of Engineering (Newton Fund UK-CIAPP\286 and TSPC1025). *(Corresponding author: Jing Xun).*

Y. Liu, J. Xun and T. Tang are with the State Key Laboratory of Traffic Control and Safety, Beijing Jiaotong University, Beijing 100044, China (e-mail: yafeiliu@bjtu.edu.cn, jxun@bjtu.edu.cn, ttang@bjtu.edu.cn).

R. Liu is with the Institute for Transport Studies, University of Leeds, Leeds, LS2 9JT, United Kingdom (e-mail: R.Liu@its.leeds.ac.uk).

C. Wei is with the School of Mechanical and Aerospace Engineering, Queen's University Belfast, Belfast, BT7 1NN, United Kingdom (e-mail: weichongfeng@gmail.com).

for VC, in dealing with coupling and decoupling processes of trains crossing the switch point from/to different tracks [5], requires consideration of the operation rules for interlocking and train route selection, which is beyond the scope of stability control for the VCTS and is therefore not covered in this study.

For the benefit of closer running within a VCTS, the small spacing can also lead to potential issues of safety (e.g., rear-end collisions) and instability (e.g., spacing fluctuations) [6]. There are two most influential factors: one is the time-varying maneuvers of the leading train caused by varying speed limits along the rail route, and the other one is the interference from neighboring trains due to disturbances. Due to the very limited spacing between trains under VC, the operation of the following trains can be adversely affected under certain conditions, and then the safety and stability of the VCTS could be influenced negatively.

One of the biggest challenges of the VCTS control problem, thus, is how to guarantee the safe and stable operation of the VCTS. To be more specific, a safe and stable VCTS means that states of following trains can stay within a certain range around an equilibrium state (e.g., desired spacing and consistent speed) and emergency braking will not be triggered, given internal interference (between trains within a VCTS) and external disturbances (due to varying track speed limits). Therefore, the key issue of achieving the safe and stable operation of the VCTS is to ensure each following train is controlled optimally and precisely to minimize interference and disturbances.

A. Literature review

The purpose of this study is to mitigate the VCTS control problem resulted from multiple trains under VC, by taking the stable control methods into consideration. In the literature, there are three main approaches for VCTS control: 1) rule-based train-following control; 2) closed-form linear feedback control; 3) constrained optimal control.

Briefly speaking, the train-following control approach is based on the car-following theory and can be used to test control algorithms and design solutions to control problems for trains [7]–[9]. A train-following model was developed in [3] to capture the train dynamics and practical operation scenarios of trains running under VC. However, such train-following control strategies are rule-based and not optimized, and the performance of the control strategies relies on fine-tuned and carefully calibrated model parameter values. The second approach, i.e., the feedback control strategy, was utilized under the concept of VC and evaluated in the context of ETCS in [10]. A linear feedback control law was formulated based on the spacing error and the speed difference between trains in the VCTS. However, it is difficult to use the feedback control method to handle constraints, e.g., control input constraints caused by traction and braking performance. This drawback limits its application in high-speed scenarios in which considerations of constrained traction and braking performance are usually needed. In order to tackle hard constraints of the control problem while guaranteeing optimality, optimal control methods, e.g., Model Predictive Control (MPC), have been widely investigated and applied, such as in solving the vehicle platoon problems [11]–[13]). A VC control system for a metro line was developed in [14] under the framework of MPC. The results showed that the computation time rises rapidly as the number of trains in convoy increases, and the stability conditions of the control method were not derived. Inspired by [14], in this paper, we propose an optimal control method for train control under VC with constraints to ensure stability between trains within a VCTS. We derive mathematical conditions for stability and provide numerical examples to illustrate how the stability regions vary with model parameter settings. A distributed MPC framework is realized for the control, to enable fast and efficient solutions to be generated.

It is also worth mentioning that there are some similarities in concepts between VCTS (or train platoon) and car platoon, and the latter has seen extensive research on longitudinal vehicular platoon control in the field of road traffic [15]–[18]. There are however three key challenges that need to be handled in the VCTS control problem and distinguish it from road vehicular platoon: (i) detailed safe braking process, (ii) restricted traction/braking performance, and (iii) variation in longitudinal speed limits.

Specifically, first, because of the lower rail-wheel adhesion, the braking distance of trains is significantly longer, e.g., 4-5km at a speed of 300km/h [3]. Thus it becomes necessary to take the detailed braking process into safety consideration. By introducing the innovative relative braking distance, the coupling dynamics of the VCTS in the safety constraint brought from the safe braking distance, however, is represented as a nonlinear coupled constraint. This results that the rule-based train-following control and the linear feedback control methods cannot handle such coupled constraints [19], and existing research either ignores this safety issue or simplifies it to obtain the feasibility of this constrained control problem. Second, the traction and braking performance of trains are limited compared to those of cars, especially at high-speed operation, leading to both restricted control range and individual constraints. If disturbances happen and these constraints are not considered in the control design, the output control force could reach saturation and not achieve the desired effect. Also, such limitations make stable control hard to be guaranteed under internal interference and external disturbances, as additional constraints would affect the feasibility and stability conditions of a controller. Third, most road vehicular platoon control problems are studied under cruising scenarios with a constant time gap policy and following the same speed limit. In HSR, speed limits on the tracks can vary significantly due to different train types, line conditions, and weather. En-route varying speed limits are endogenous disturbances in the VCTS control problem, leading to changing maneuvers of the leading train and variable equilibrium states.

B. Proposed approach and contributions

To overcome the abovementioned issues, this paper proposes a distributed MPC (DPMC)-based method for the VCTS control problem, aiming to mathematically derive feasibility and stability conditions with individual and coupled constraints. To this end, a state-space model is formulated to

TABLE I
SELECTED LITERATURE ON THE RESEARCH OF TRAIN PLATOON CONTROL

Publications	Methods	System properties		Theoretical properties	
		Individual constraints	Coupled constraints	Feasibility	Stability
[3]	Train-following model	Speed limits and control force	None	Not guaranteed	Not guaranteed
[10], [20]–[22]	State-feedback control	None	None	Not guaranteed	Guaranteed and proved
[23]	Model predictive control	Speed limits and control force	Safety constraint of constant braking distance	Guaranteed	Guaranteed
[14]	Model predictive control	Speed limits and control force	Safety constraint of relative braking distance only for terminal states	Guaranteed	Not guaranteed
This study	Distributed model predictive control	Speed limits and control force	Safety constraint of relative braking distance for all predicted states	Guaranteed and proved	Guaranteed and proved

describe the virtually coupled train dynamics. An optimal control formulation is further constructed into the DMPC framework, which enables to deal with the coupled constraint of safety braking distance and the individual constraints of speed limit variations and restricted traction/braking performance. Through designing the terminal constraint set and the terminal controller of the DMPC algorithm, the feasibility and stability of this constrained optimal control problem are guaranteed. For rigor, sufficient conditions of feasibility and stability are mathematically proved and derived. Numerical experiments are conducted to confirm the effectiveness of the proposed method.

Compared with existing research on train platoon control, as shown in Table I, this study makes major contributions from three aspects presented as follows. 1) Compared to the existing VCTS control methods which omit safety issues or simplify safety constraints, this study represents the braking distance as a coupled safety constraint in the optimal control formulation and ensures the feasibility through deliberately designing the DMPC algorithm, which allows trains in the VCTS to run at the minimum spacing while ensuring safety. 2) A distributed MPC framework is realized in this study to handle the coupled constraint shared between two adjacent trains in the VCTS. The original VCTS control problem is decomposed into sub-problem since trains as sub-systems can be dynamically decoupled and have independent controllers. The proposed DMPC algorithm also allows efficient solutions and facilitates practical applications, especially when the VCTS system is expanded with more trains. 3) While existing research has focused on the constraint brought by speed limits, the stability of the VCTS control system under such variable conditions is not yet discussed. In this study, the asymptotical stability is achieved on the basis of the derived sufficient conditions under the proposed DMPC algorithm, under disturbances caused either by the initial speed differences and spacing errors in VCTS, or by the variable speed limits that trains in the VCTS need to respond to.

The rest of this paper is organized as follows. Section II presents the state-space formulation, constraints, and the objective for virtually coupled train control. Section III describes the formulation of the constrained optimal control problem for VCTS in a DMPC framework and presents the derived feasibility and stability conditions. In section IV, numerical experiments are conducted to illustrate the effectiveness of the proposed method. Finally, the conclusion and future research are discussed in section V.

TABLE II
SYMBOLS AND NOTATIONS

Symbols	Units	Descriptions
N	-	Number of trains in the VCTS
D_d	m	Desired spacing
$D_{\min}$	m	Safety margin
D_L	m	Length of a train
s_i	m	Absolute position
v_i	m/s	Velocity
$v_{\lim}$	m/s	Speed limit
$U_{\min}, U_{\max}$	m/s^2	Minimum and maximum control force
$\mathbb{U}$	-	Control variable set
$\mathcal{X}_{\text{safe}}$	-	Safety constraint set
x_i	-	State of a train
x_i^*	-	Predicted state of a train
u_i	m/s^2	Nominal control force
u_i^e	m/s^2	Difference of control forces
u^*	m/s^2	Optimal control force
(p_1, p_2, q_1, q_2, R)	-	Weight coefficients
T_p	-	Prediction horizon
t_k	-	Time step
δ	s	Sample time
π^f	-	Terminal controller
$\mathcal{X}_f$	-	Terminal constraint set

II. MATHEMATICAL FORMULATION FOR VIRTUALLY COUPLED TRAIN CONTROL

A. Symbols and notations

The relevant symbols and notations are listed in Table II to describe the problem more clearly.

B. Train dynamics

The longitudinal train dynamics is modelled by taking the traction/braking system, the aerodynamic drag, the rolling resistance, and the ramp resistance into account [24], [25]. Therefore, the train dynamics can be formulated as:

$$\begin{cases} \dot{s}_i(t) = v_i(t), \\ \dot{v}_i(t) = \bar{u}_i(t) - \dfrac{1}{m_i}(r_i(v_i(t)) + g_i(s_i(t))), \end{cases} \tag{1}$$

where i is the train index number; $s_i(t)$, $v_i(t)$ are the position and the speed of train i, respectively; m_i is the mass of train i;

$\bar{u}_i(t)$ denotes the control force per unit mass, i.e., the desired acceleration for train i; $r_i(v_i(t))$ represents the combination of the track resistance and air drag resistance; and $g_i(s_i(t))$ is the ramp resistance. Note that factors that affect different resistances during train operation are complicated. In this case, $r_i(v_i(t))$ is usually calculated by an empirical formula called the Davis equation as:

$$r_i(v_i(t)) = c_0 + c_1 v_i(t) + c_2 v_i^2(t), \tag{2}$$

where c_0, c_1 and c_2 are Davis coefficients that may change with different trains and line conditions. The ramp resistance is the force caused by the track gradient (positive for upgrade and negative for downgrade). When the gradient is small, the force can be approximated as follows:

$$g_i(s_i(t)) = m_i \varrho \theta(s_i(t)), \tag{3}$$

where θ is the track gradient, measured in terms of the ratio of the vertical rise to the horizontal distance, whose value depends on the current position of the train and the route layout, and ϱ denotes the gravitational constant.

According to [26], linearization techniques are usually used in platoon control systems for theoretical convenience. Here we adopt the linearization near the equilibrium point and use the same form as [23], as the speed profile $v_0(t)$ of the leading train (the first train of the VCTS with index 0) is pre-determined. According to (1) and the Taylor expansion, the linearized dynamic equation around the equilibrium state where $v_0(t) = v_1(t) = ... = v_N(t)$ is obtained by

$$\begin{cases} \dot{s}_i(t) = v_i(t), \\ \dot{v}_i(t) = u_i(t) - h_i(t) v_i(t) - l_i(t). \end{cases} \tag{4}$$

Here $u_i(t) = \bar{u}_i(t) - \frac{g_i(s_i(t))}{m_i}$, $h_i(t) = \frac{c_1 + 2c_2 v_0(t)}{m_i}$ and $l_i(t) = \frac{c_0 - c_2 v_0^2(t)}{m_i}$ for each train $i = 0, 1, ..., N-1$. Note that the control variable $\bar{u}_i(t)$ is rewritten as $u_i(t)$ for simplicity; this is because the line profile is pre-defined and the ramp resistances could be calculated beforehand to reduce online computational time.

C. State-space model for the virtually coupled train set (VCTS)

To investigate the control problem of a VCTS, we first formulate a state-space model to describe the dynamics of, and the interconnections among, the virtually coupled trains. A VCTS with T2T communication is displayed in Fig. 2 to illustrate the composition and the communication topology. Here we consider a VCTS composed of N trains moving along a railway line. In the scenario under investigation, trains are organized in order without overtaking, sharing their state information (e.g., position, velocity, and acceleration) with neighboring trains. The onboard equipment integrated with the speedometer and balise receiver allows each train to attain its absolute position, velocity, and acceleration. A reference trajectory is imposed on the leading train (the first train of the VCTS with index 0).

In our model, we define the state of train i in a VCTS as:

$$x_i(t) = [\Delta s_i, \Delta v_i]^T, \tag{5}$$

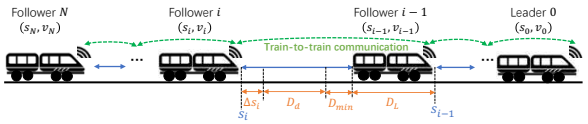

Fig. 2. Illustration of the composition and the communication topology in a virtually coupled train set.

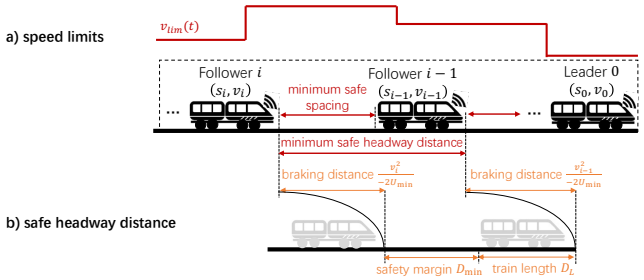

Fig. 3. Illustration of key railway features: the variable speed limits and the safe braking distance.

in which $\Delta s_i = s_{i-1}(t) - s_i(t) - D_d - D_L - D_{\min}$, as shown in Fig. 2, denotes the deviation from the desired constant spacing D_d with respect to the preceding train; D_L is the length of each train and $D_{\min}$ is the safety margin; $\Delta v_i = v_{i-1}(t) - v_i(t)$ is the speed difference with respect to the preceding train. Here we assume trains have the same mass $m_i = m$, thus $h_i(t)$ in Eq. (4) can be simplified as $h(t)$ for $i = 0, 1, ..., N-1$. Then, the state equation of train i is obtained by substituting Eq. (4)

$$\dot{x}_i(t) = A(t) x_i(t) + B u_i^e(t), \tag{6}$$

where

$$A(t) = \begin{bmatrix} 0 & 1 \\ 0 & -h(t) \end{bmatrix}, B = \begin{bmatrix} 0 \\ 1 \end{bmatrix}, u_i^e(t) = -u_i(t) + u_{i-1}(t).$$

D. Individual and coupled constraints

As shown in Fig. 3, variable speed limits, caused by line and environmental conditions, are endogenous disturbances in the VCTS control problem, leading to varying maneuvers of trains and variable equilibrium states. For each train in the VCTS, the individual constraint of speed limits is written as:

$$0 \le v_i(t) \le v_{\lim}(s_i(t)), \tag{7}$$

where $v_{\lim}(s_i(t))$ is the speed limit at location $s_i(t)$. Due to train traction/braking characteristics, the following constraint on the control force is also considered for each train:

$$U_{\min} \le u_i(t) \le U_{\max}, \tag{8}$$

where $U_{\min}$ and $U_{\max}$ denotes the maximum braking and maximum traction force respectively.

Additionally, in Fig. 3, the safe spacing of train i with respect to its predecessor is constrained by the relative braking distance. We can see that the minimum safe spacing can be described as

$$s_{\text{safe}} = D_{\min} + \max\left(\frac{v_i^2(t)}{-2U_{\min}} - \frac{v_{i-1}^2(t)}{-2U_{\min}}, 0 \right) \tag{9}$$

where v_i is the velocity of train i, $U_{\min}$ is the maximum deceleration, $v_i^2(t)/U_{\min}$ is the emergency braking distance of train i, $D_{\min}$ is a safety margin that related to the positioning error of the train. Specifically, this minimum safe spacing has two implications. One is that if the braking distance of train $i-1$ is longer than that of train i, i.e., $v_{i-1}^2(t)/U_{\min} - v_i^2(t)/U_{\min} < 0$, the safe spacing between them could be just larger than the sum of the safety margin and the train length, i.e., $D_{\min} + D_L$. The other one is that if the situation is reversed, i.e., $v_{i-1}^2(t)/U_{\min} - v_i^2(t)/U_{\min} > 0$, an additional term relating to braking distance difference should be considered to avoid rear-end collision. With the minimum safe spacing in Eq. (9), the safety constraint between two adjacent trains within the VCTS can be denoted by:

$$s_{i-1}(t) - s_i(t) - D_L \geq s_{\text{safe}}, \tag{10}$$

where D_L is the length of a train. Eq. (10) ensures that the following train i can brake to stop without the rear-end collision whenever the preceding train $i-1$ starts braking until standstill.

Eq. (10) includes a non-linear term $\max(\cdot)$. In order to transfer the inequality of (10) into linear forms and to generalize constraints (7)-(10), we denote the following constraint sets:

Control variable set:

$$u_i(t) \in \mathbb{U} = \{u_i : U_{\min} \leq u_i \leq U_{\max}\}, \tag{11}$$

Safety constraint set:

$$x_i(t) \in \mathcal{X}_{\text{safe}} = \{x_i : \phi_j(x_i) \geq 0, j = 1, 2, ..., 4\}, \tag{12}$$

where

$$\begin{aligned}
\phi_1(x_i) &= s_{i-1}(t) - s_i(t) - \frac{v_{i-1}^2(t)}{2b_{i-1}} + \frac{v_i^2(t)}{2b_i} - D_{\min} - D_L, \\
\phi_2(x_i) &= s_{i-1}(t) - s_i(t) - D_{\min} - D_L, \\
\phi_3(x_i) &= v_i(t), \\
\phi_4(x_i) &= v_{\lim} - v_i(t),
\end{aligned}$$

u_i is the control variable described in Eq. (4), and x_i is the state of train i described in Eq. (5).

E. Control objective

In this study, the goal is to regulate the spacing and minimize speed difference between trains in the VCTS and to achieve stable operation at the equilibrium state $x_{i,e} = (0,0)^T$, i.e.,

$$\begin{cases} x_i(t) = (0,0)^T, \\ \dot{x}_i(t) = (0,0)^T, \forall t > 0 \end{cases} \tag{13}$$

which means that there is no deviation from the desired spacing and no speed difference between adjacent trains.

To achieve this goal, the cost function can be defined by

$$\Psi_i(x_i(t_k), u_i(t_k)) = L_i(x_i(t_k), u_i(t_k)) + G_i(x_i(t_k + T_p)), \tag{14}$$

where

$$L_i(x_i(t_k), u_i(t_k)) = \|x_i(t_k)\|_Q^2 + \|u_i^e(t_k)\|_R^2, \tag{15}$$

$$G_i(x_i(t_k + T_p)) = \|x_i(t_k + T_p)\|_P^2. \tag{16}$$

The cost function in Eq. (14) consists of two components as suggested by [17] and [15]. The first component is the running cost presented in Eq. (15), representing the deviation from the equilibrium state and differences of control variables, where $\|\cdot\|_Q^2$ denotes the Euclidean norm with its weight coefficient Q as the subscript. The second component is the terminal cost in Eq. (16) that penalizes the deviation of the terminal state from the equilibrium state. Eq. (16) can be used to restrict the terminal state at the end of the prediction horizon T_p and to guarantee stability. This terminal cost will be further discussed and designed in the next section since it plays an important role in the finite horizon optimal control problem. The positive-definite matrices $P = \text{diag}\{p1, p2\}$ and $Q = \text{diag}\{q1, q2\}$ are two-dimensional weight coefficients as x_i in Eq. (5) is a two-dimensional variable. R is a one-dimensional positive weight coefficient.

III. Optimal control formulation in distributed model predictive control framework

A. General optimal control formulation

The VCTS control problem is formulated as a constrained optimal control problem in the MPC framework. The MPC has the ability to handle control systems with hard constraints on controls and states [27]. There are mainly three control schemes under the general MPC framework: centralized MPC, decentralized MPC, and distributed MPC [28]. These schemes could be applied to different types of control systems. For the complicated large-scale system, the centralized control scheme can lead to a considerable amount of online calculation and negatively affect the performance for real-time control [16]. By dividing the whole-system control into a series of subsystem control problems and solving them separately, the decentralized control scheme can reduce the model complexity. However, the correlation between subsystems is ignored in decentralized MPC, resulting in degradation of the overall performance and even causing instability to the system [28]. DMPC addresses these two features (i.e., sub-systems and correlations between sub-systems) together and gives a solution for the control problem of interconnected systems.

For the VCTS control system, each train in the VCTS is a sub-system where the strong correlation (e.g., coupled safety constraints and information exchange) is in between. To tackle the above limitations of the centralized and decentralized control schemes and to meet the real-time performance of train control systems, a distributed MPC scheme is realized for the VCTS control problem in this study. DPMC is applicable because trains have independent controllers and can obtain both state and control information of each other via the T2T communication link. Furthermore, the distributed control mechanism allows for easy expansion and reduction of the VCTS system, especially when trains merge into or leave the VCTS.

In the DMPC framework, we introduce $(x_i(\tau|t_k), u_i(\tau|t_k))$ to denote the state variable and the control variable at time interval $\tau \in [t_k, t_{k+1})$ where $t_{k+1} - t_k = \delta < T_p$ and δ is the sample time. $X_i^*(t_k) = [x_i^*(t_k + \delta|t_k), ..., x_i^*(t_k + T_p|t_k)]$ and $U_i^*(t_k) = [u_i^*(t_k|t_k), u_i^*(t_k + \delta|t_k), ..., u_i^*(t_k + T_c - \delta|t_k)]$

represent the optimal predicted trajectory and the optimal control sequence, respectively. T_p and T_c denote the prediction horizon and the control horizon, respectively. For the standard MPC framework and to reduce the calculation complexity in practical applications, $T_c \leq T_p$ is often implemented and the control variables are assumed to be zero for all $\tau \in [t_k + T_c, t_k + T_p]$, i.e., $u_i(\tau|t_k) = 0$ [29], [30]. In control of road vehicles, a prediction time horizon is typically set as $T_p = 3$ sec to cover the sightline of human drivers. In railway, however, the extent covered by the horizon should be larger than that of road vehicles due to the high operation speed, leading to a relatively long prediction horizon.

Specifically, the finite horizon constrained optimal control problem for the VCTS is formulated in a DMPC scheme as follows, considering minimizing the spacing deviation and the speed difference and improving the control efficiency as objectives, subject to safe constraints and traction/braking power limits:

$$\begin{aligned}
&\min_{u_i(\tau|t_k)} J_i\left(x_i\left(t_k\right), u_i\left(t_k\right)\right) \\
&\qquad = \int_{t_k}^{t_k+T_p} \Psi_i\left(x_i\left(\tau|t_k\right), u_i\left(\tau|t_k\right)\right) d\tau \qquad (17)\\
&\text{s.t.} \quad \dot{x}_i\left(\tau|t_k\right) = A\left(\tau|t_k\right) x_i\left(\tau|t_k\right) + B u_i^e\left(\tau|t_k\right), \qquad (17a)\\
&\qquad x_i\left(t_k|t_k\right) = x_i\left(t_k\right), \qquad (17b)\\
&\qquad x_i\left(\tau|t_k\right) \in \mathcal{X}_{\text{safe}}\ , \qquad (17c)\\
&\qquad u_i\left(\tau|t_k\right) \in \mathbb{U}, \qquad (17d)\\
&\qquad x_i\left(t_k + T_p|t_k\right) \in \mathcal{X}_f, \qquad (17e)
\end{aligned}$$

where Eq. (17) is the objective function and Ψ_i is the cost function as described in Eq. (14); constraint (17a) is the state equation as mentioned in Eq. (6); constraint (17b) describes the initial state; constraint (17c) represents the coupled safety constraints according to Eq. (12); constraint (17d) denotes the admissible set of control variables introduced in Eq. (11); constraint (17e) is the terminal constraint and is related to feasibility and stability which will be further discussed and designed in the following section. Note that this optimal control formulation is formulated in a continuous-time form because the train dynamics Eq. (1) and the state transition equation Eq. (6) show that the VCTS control system can be mathematically described as a continuous-time system. For more details of the continuous form of MPC, readers are referred to [27].

The implementing details and the solution procedure of the above VCTS control problem are provided in Algorithm 1. Unlike the MPC method used in [14] where the safety constraint was only considered in the terminal step to ensure the feasibility, the proposed algorithm is designed to guarantee both feasibility and stability of the DMPC controller with nonlinear constraints at all time steps within the prediction horizon. Therefore, the proposed algorithm is more robust and stable under disturbances. Moreover, the distributed control algorithm is implemented sequentially, where the preceding train $i-1$ completes its calculation and then transmits its state information to the following train i. Under this strategy, the control problem can be decomposed into subproblems and solved sequentially along the VCTS. For train i, it can receive the information from its predecessor, i.e., $(s_{i-1}(t), v_{i-1}(t), u_{i-1}(t))$. Then, the safety constraint in Eq. (10) can be decoupled and handled for train i, instead of solving the coupled constraint for two neighboring trains simultaneously, which reduces the complexity of the control problem and improves the algorithm efficiency.

Algorithm 1

1: Initialize states of all trains in the VCTS at time $t_k = 0$ and assume the DMPC problem in Eq. (17) is feasible at the initial time; set the speed profile for the leading train and make it start to run; set the train number $i = 1$.
2: At time t_k, assign the initial state using Eq. (17b); calculate the optimal control sequence of train i, $U_i^*(t_k) = [u_i^*(t_k|t_k), u_i^*(t_k+\delta|t_k), \ldots, u_i^*(t_k+T_c-\delta|t_k)]$, by solving the problem in Eq. (17), and derive its predicted trajectory, $X_i^*(t_k) = [x_i^*(t_k+\delta|t_k), \ldots, x_i^*(t_k+T_p|t_k)]$, according to Eq. (17a).
3: Implement the first item $u_i^*(t_k|t_k)$ in $U_i^*(t_k)$ to control train i at time interval $[t_k, t_{k+1})$, and transmit $X_i^*(t_k)$ and $U_i^*(t_k)$ to train $i+1$ via T2T communication.
4: Check for $i < N-1$. If yes, update the train number $i = i+1$ and go back to step 2. If not, go to step 5.
5: Check if the simulation ends. If yes, stop. If not, shift the prediction horizon, update the time $t_k = t_{k+1}$ and set the train number $i = 1$.
6: Check the feasibility of the problem to ensure it is solvable at time t_{k+1}. For all $i \leq N-1$, use $U_i^*(t_k)$ and the terminal controller $\pi^f(\cdot)$ to construct a feasible control sequence $\tilde{U}_i(t_{k+1}) = \left[u_i^*(t_k+\delta|t_k), \ldots, u_i^*(t_k+T_c-\delta|t_k), \pi^f(t_{k+1})\right]$; calculate the feasible predicted trajectory $\tilde{X}_i(t_{k+1})$ using $\tilde{U}_i(t_{k+1})$.
7: Check if $\tilde{X}_i(t_{k+1})$ stays in the admissible sets (17d) and (17e). If yes, the problem is feasible and go back to step 2. If not, stop.

B. Design of terminal controller and terminal constraint set

In order to guarantee the iterative feasibility and stability of the VCTS control problem (17) in the proposed DMPC algorithm, a terminal controller and a terminal constraint set need to be deliberately designed. Specifically, as described in Algorithm 1, the terminal controller is used to construct a feasible control sequence and then to calculate a feasible state trajectory; this trajectory will satisfy the terminal constraint and guarantee the feasibility of the problem. Moreover, these two components (i.e., the terminal controller and the terminal constraint set) are also designed to make the DMPC algorithm for the VCTS control problem asymptotic stable, which would be further proved in the following section. For theoretical convenience, here the prediction horizon and the control horizon are assumed to be the same, i.e., $T_p = T_c$. According to [31] and [27], the detailed definition for them is as follows:

Definition 1. *(Terminal controller and Terminal Constraint Set)* For the DMPC problem (17), the terminal controller $\pi^f(\cdot)$ and the terminal constraint set $\mathcal{X}_f$ are such that if $x_i(t_k + T_p|t_k) \in \mathcal{X}_f$, then, for any $\tau \in (t_k + T_p, t_{k+1} + T_p]$, by implementing the terminal controller $\pi^f(\tau|t_k) = \pi^f(x_i(t_k + T_p|t_k))$, it holds that

$$\pi^f\left(\tau|t_k\right) \in \mathbb{U}, \qquad (18)$$

$$x_i\left(\tau|t_k\right) \in \mathcal{X}_f, \qquad (19)$$

$$\dot{G}_i\left(x_i\left(\tau|t_k\right)\right) + L_i\left(x_i\left(\tau|t_k\right), u_i\left(\tau|t_k\right)\right) \leq 0. \qquad (20)$$

From the above definition, it can be observed that the terminal controller π^f should satisfy the control variable constraint $\mathbb{U}$ in the condition (18) at all times since it is a control variable for each train in the VCTS. For the terminal constraint set $\mathcal{X}_f$, it is defined as an invariant set for the terminal controller π^f [17]. This means that if the condition (19) holds at time t_k+T_p, it holds at time interval $(t_k+T_p, t_{k+1}+T_p]$ for all π^f satisfying the condition (18). This ensures that the terminal constraint is always satisfied under the terminal control variable π^f if states x_i are located in the terminal constraint set $\mathcal{X}_f$. Furthermore, conditions (18)-(20) contribute to the feasibility and stability of the DMPC problem, which will be further discussed and proved in the next section. In this section, the terminal controller and the terminal constraint set are designed according to conditions depicted in Definition 1.

The following proposition provides a terminal constraint set and a terminal controller for the DMPC problem (17), suggested by [31]. However, due to the coupled safety constraints and the distinct transition dynamics for this VCTS control problem, both the designed components and the derived conditions are distinct from previous studies.

Proposition 1. According to Definition 1, for the DMPC problem (17), $\mathcal{X}_f = \mathcal{X}_{\text{safe}} \cap \{x_i(\tau|t_k) : \xi_1 \le Hx_i \le \xi_2\}$ is a terminal constraint set for the terminal controller

$$\pi^f(\tau|t_k) = K_f x_i(\tau|t_k) + u_{i-1}(\tau|t_k), \tag{21}$$

where $K_f = [k_s, k_v]$, k_s and k_v are positive control gains, $H = [0,1]$, $\xi_1 = \frac{U_{\min}-u_{i-1}}{k_v}$, $\xi_3 = \frac{U_{\max}-u_{i-1}}{k_v}$ and $\tau \in (t_k + T_p, t_{k+1} + T_p]$, with the parameters satisfying

$$k_s = 0, k_v \in [\alpha_1, \alpha_2], \tag{22}$$

$$R \le \frac{q_1 p_2^2}{q_1 q_2 - 2h q_1 p_2 - p_1^2}, \tag{23}$$

$$q_1 q_2 - 2h q_1 p_2 - p_1^2 \ge 0, \tag{24}$$

where $\alpha_{1,2} = \frac{\left(q_1 p_2 \pm \sqrt{q_1^2 p_2^2 - q_1 R\left(q_1 q_2 - 2h q_1 p_2 - p_1^2\right)}\right)}{q_1 R}$, p_j and q_j $(j = 1, 2)$ are the entries of positive-definite matrices P and Q, and R is a positive real number.

Proof. First, according to Definition 1, the proposed terminal controller π^f in Eq. (21) should satisfy the condition (18), resulting the following condition:

$$U_{\min} \le \pi^f(\tau|t_k) = K_f x_i(\tau|t_k) + u_{i-1}(\tau|t_k) \le U_{\max}, \tag{25}$$

which could be further transferred to

$$\xi_1 \le Hx_i(\tau|t_k) \le \xi_2, \tag{26}$$

where $H = [0,1]$, $\xi_1 = \frac{U_{\min}-u_{i-1}}{k_v}$ and $\xi_2 = \frac{U_{\max}-u_{i-1}}{k_v}$. This means that the terminal state needs to be within a certain range to make the controller meet the constraint. In addition, as the safety constraints should be satisfied for all states at all times, the proposed terminal constraint set $\mathcal{X}_f$ is designed to be located in the safety constraint set $\mathcal{X}_{\text{safe}}$, i.e., $\mathcal{X}_f \subseteq \mathcal{X}_{\text{safe}}$. Therefore, by setting $\mathcal{X}_f = \mathcal{X}_{\text{safe}} \cap \{x_i(\tau|t_k) : \xi_1 \le Hx_i \le \xi_2\}$, the condition (18) in Definition 1 and the safety constraint $\mathcal{X}_{\text{safe}}$ could be all satisfied if $x_i(\tau|t_k) \in \mathcal{X}_f$.

Next, according to the condition (19) in Definition 1, the proposed $\mathcal{X}_f$ should be an invariant set for the terminal controller π^f. Moreover, the safety constraint set $\mathcal{X}_{\text{safe}}$ has been proved as an invariant set [11]. Thus, the relation $\mathcal{X}_f \subseteq \mathcal{X}_{\text{safe}}$ indicates that $\mathcal{X}_f$ could be also invariant if the terminal state $x_i(\tau|t_k)$ still locates in $\mathcal{X}_f$ after the transition with the terminal controller π^f. By choosing the terminal cost $G_i(x_i(\tau|t_k))$ in Eq. (16) as Lyapunov function, suggested by [31], the derivative of the Lyapunov function by substituting the terminal controller Eq. (21) with respect to time τ could be obtained as:

$$\begin{aligned}\left|\dot{G}_i\left(x_i(\tau|t_k)\right)\right| &= \left|(A+BK_f)^T P + P(A+BK_f)\right| \\ &= \left|\begin{array}{cc} 0 & p_1 - p_2 k_s \\ p_1 - p_2 k_s & -2p_2(k_v+h) \end{array}\right| = -(p_1 - p_2 k_s)^2 \le 0.\end{aligned} \tag{27}$$

This implies that the terminal state will asymptotically approach the equilibrium state $x_{i,e} = (0,0)^T$, which is also located in the set of $\mathcal{X}_f$, under the control of π^f. This ensures that the ultimate terminal state will always fall in the terminal constraint set $\mathcal{X}_f$ if the terminal state consistently originates from $\mathcal{X}_f$ for all admissible π^f. Therefore, the proposed terminal constraint set $\mathcal{X}_f$ is an invariant set for the proposed terminal controller π^f, and conditions (18)-(19) in Definition 1 are satisfied.

Furthermore, according to Definition 1, the condition (20) should be calculated as follows by substituting Eq. (15) and (16):

$$\begin{aligned}&(\dot{G}_i + L_i)\left(x_i(\tau|t_k), \pi^f(\tau|t_k)\right) = x_i^T((A-BK_f)^T P \\ &+ P(A-BK_f) + Q + K_f^T R K_f) x_i \le 0.\end{aligned} \tag{28}$$

To guarantee that the above inequality holds, we have

$$\begin{aligned}&\left|(A+BK_f)^T P + P(A+BK_f) + Q + K_f^T R K_f\right| \\ &= \left|\begin{array}{cc} q_1 + Rk_s^2 & p_1 - p_2 k_s + Rk_s k_v \\ p_1 - p_2 k_s + Rk_s k_v & Rk_v^2 - 2p_2(k_v+h) + q_2 \end{array}\right| \\ &= \left(q_1 + Rk_s^2\right)\left(Rk_v^2 - 2p_2(k_v+h) + q_2\right) \\ &\quad - (p_1 - p_2 k_s + Rk_s k_v)^2 \le 0.\end{aligned} \tag{29}$$

Here we denote $k_s = 0$ to simplify the above inequality as k_s is a controller gain that could be adjusted. Therefore, the sufficient conditions (23) and (24) could be derived by calculating

$$q_1\left(Rk_v^2 - 2p_2(k_v+h) + q_2\right) - p_1^2 \le 0, \tag{30}$$

which is a quadratic inequality. The left side of Eq. (30) can be recognized as a quadratic function of k_v whose parabola opens upwards and vertex is on the right side of the y-axis. Roots of the quadratic function are derived as:

$$\alpha_{1,2} = \frac{\left(q_1 p_2 \pm \sqrt{q_1^2 p_2^2 - q_1 R(q_1 q_2 - 2h q_1 p_2 - p_1^2)}\right)}{q_1 R}. \tag{31}$$

Furthermore, the vertex of this parabola is needed to be in the forth quadrant of the axis, and the roots should be positives

because k_v is a positive control gain, i.e., $k_v \geq 0$. To achieve this, conditions (23)-(24) can be derived from Eq. (31) as:

$$\begin{cases} q_1^2 p_2^2 - q_1 R\left(q_1 q_2 - 2h q_1 p_2 - p_1^2\right) \geq 0, \\ q_1 q_2 - 2h q_1 p_2 - p_1^2 \geq 0. \end{cases} \tag{32}$$

Then, if k_v satisfies the condition (22) and conditions (23)-(24) hold, the inequality (30) can be satisfied.

On the basis of above sufficient conditions, the condition (20) in Definition 1 is satisfied. Therefore, the proposed terminal constraint set $\mathcal{X}_f$ and terminal controller π^f meet all the requirements in Definition 1. □

Remark 1. Different from the works done by [11] and [14], this study further expands the feasibility and stability conditions of the DMPC controller featured with coupled safety constraints through designing the terminal constraint set and the terminal controller. Specifically, the study in [11] proved that the safety constraint set $\mathcal{X}_{\text{safe}}$ in such form Eq. (12) is a robust controlled invariant set for the control variable set Eq. (11). This ensures that the safety constraint is always satisfied under the limited control variable if the states are located in the safety constraint set $\mathcal{X}_{\text{safe}}$, which addresses the feasibility of the MPC problem. This conclusion could be applied to ensure the feasibility [14]; however, it still cannot guarantee stability, since the states may not approach the equilibrium state asymptotically under such nonlinear coupled constraints. Additionally, unlike [11], the safety constraint set is not considered as the worst case resulted from uncertain ramp resistances in road transport. Reasons can be explained from two perspectives: first, the spacing between adjacent trains would inevitably become very large due to the stricter safety constraint in high-speed scenarios; second, as the line profile is foreknown in railway, the ramp resistances could be calculated as a certain value in each position throughout the line. Thus, the results and proofs in [11] cannot be directly applied to solve the high-speed VCTS control problem.

Remark 2. As shown in the derived sufficient conditions (22)-(24), the parameters of the DMPC controller should be selected in line with the conditions. As P, Q and R are adjustable weight coefficients associated with the objective function (14), they could be fine-tuned to achieve expected performance as long as satisfying the above sufficient conditions, e.g., $R = 0.5$ suggested in [15] and $p_1 = p_2 = 0.5$ suggested in [31]. In addition, terminal control gain k_v could be selected according to Eq. (30); however, it is recommended to choose the minimum value to make the terminal region as large as possible since k_v directly affects $\mathcal{X}_f$.

C. Feasibility and stability

Based on the design of the terminal constraint set and the terminal controller as well as the derived sufficient conditions, the feasibility and stability of the DMPC algorithm for the VCTS control problem are discussed in this section.

Proposition 2. The DMPC Algorithm 1 for the VCTS control problem in Eq. (17) is feasible for all $t_k > t_0$ if this problem is initially feasible at t_0 with the terminal constraint set $\mathcal{X}_f$ and the terminal controller π^f.

Proof. Assume that the VCTS control problem in Eq. (17) is feasible and can be solved at t_k, then an optimal control sequence can be obtained as $U_i^*(t_k) = [u_i^*(t_k|t_k), u_i^*(t_k + \delta|t_k), \ldots, u_i^*(t_k + T_c - \delta|t_k)]$. Here we assume that $T_c = T_p$ to simplify theoretical analysis, and $T_c \leq T_p$ can be set in practical applications for the reduction of computation time. By implementing the control sequence, the states could be predicted by the optimal trajectory $X_i^*(t_k) = [x_i^*(t_k + 1|t_k), \ldots, x_i^*(t_k + T_p|t_k)]$ and finally enter the terminal constraint set $\mathcal{X}_f$, i.e., $x_i^*(t_k+T_p|t_k) \in \mathcal{X}_f$. From Definition 1 and Proposition 1, at t_{k+1}, there exists a feasible control sequence, $\tilde{U}_i(t_{k+1}) = [u_i^*(t_k + \delta|t_k), \ldots, u_i^*(t_k + T_c - \delta|t_k), \pi^f(t_{k+1})]$, that could drive the feasible states to eventually enter the terminal invariant set $\mathcal{X}_f$, i.e., $x_i^*(t_{k+1}+T_p|t_{k+1}) \in \mathcal{X}_f$, while satisfying the constraints. This indicates the feasibility of the optimal control problem at t_{k+1}. Thus, it can be proved that if this problem is feasible at initial time t_0, then the feasibility can be satisfied for all $t_k > t_0$ using induction. □

Before proving the stability, it needs to clarify definitions and types of stability. For a vehicular platoon control problem, local stability and string stability are mostly studied [17], [18]. In detail, the local stability means that states of the following train can stay in a certain range around an equilibrium state (e.g., the desired spacing and consistent speed) even with interference and disturbances. Furthermore, the asymptotical local stability represents that deviations of states from the equilibrium state diminish asymptotically with time. In this case, the states finally stay steadily at the equilibrium state. Nevertheless, even if the local stability of an individual following train is guaranteed, a small disturbance could be amplified upstream as the length of the platoon increases [26]. The string stability ensures that disturbances of system states are attenuated upstream; this is, uniform boundedness of system states [32]. Here we address the asymptotical local stability of the VCTS control.

Proposition 3. The DMPC Algorithm 1 for the VCTS control problem in Eq. (17) is asymptotically local stable, i.e., the system states (5) asymptotically approach the equilibrium state $x_{i,e} = (0, 0)^T$, if the algorithm is feasible and sufficient conditions (22)-(24) are satisfied.

Proof. For the VCTS control problem described in Eq. (17), the optimal cost function $J_i^*(t_k)$ is chosen as the Lyapunov function based on Eq. (17), i.e.,

$$\begin{aligned} J_i^*(t_k) &= J_i^*(x_i^*(t_k), u_i^*(t_k)) \\ &= \int_{t_k}^{t_k+T_p} L_i\left(x_i^*(\tau|t_k), u_i^*(\tau|t_k)\right) d\tau + G_i\left(x_i^*(t_k + T_p|t_k)\right). \end{aligned} \tag{33}$$

Thus the asymptotical stability could be proved if $J_i^*(t_{k+1}) - J_i^*(t_k) \leq 0$.

First, we construct a suboptimal cost function $J_i(t_{k+1})$ for t_{k+1} using a feasible control sequence $\tilde{U}_i(t_{k+1}) = \left[u_i^*(t_k + \delta|t_k), \ldots, u_i^*(t_k + T_c - \delta|t_k), \pi^f(t_{k+1})\right]$, then we

have the relation:

$$\begin{aligned} J_i\left(t_{k+1}\right) &= \int_{t_{k+1}}^{t_k+T_p} L_i\left(x_i^*(\tau|t_k), u_i^*(\tau|t_k)\right) d\tau \\ &+ \int_{t_k+T_p}^{t_{k+1}+T_p} L_i\left(x_i(\tau|t_{k+1}), u_i(\tau|t_{k+1})\right) d\tau \\ &+ G_i\left(x_i(t_{k+1}+T_p|t_{k+1})\right) \\ &= J_i^*\left(t_k\right) - \int_{t_k}^{t_{k+1}} L_i\left(x_i^*(\tau|t_k), u_i^*(\tau|t_k)\right) d\tau \\ &+ \int_{t_k+T_p}^{t_{k+1}+T_p} L_i\left(x_i(\tau|t_{k+1}), u_i(\tau|t_{k+1})\right) d\tau \\ &- G_i\left(x_i^*(t_k+T_p|t_k)\right) + G_i\left(x_i(t_{k+1}+T_p|t_{k+1})\right). \end{aligned} \tag{34}$$

Here we assume that $T_p = T_c$. From Definition 1 and Proposition 1, if conditions (22)-(24) are satisfied, the condition (20) holds. By integrating the condition (20) over interval $[t_k + T_p, t_{k+1} + T_p]$, we get

$$\begin{aligned} &G_i\left(x_i(t_{k+1}+T_p|t_{k+1})\right) - G_i\left(x_i(t_k+T_p|t_{k+1})\right) \\ &+ \int_{t_k+T_p}^{t_{k+1}+T_p} L_i\left(x_i(\tau|t_{k+1}), u_i(\tau|t_{k+1})\right) \le 0. \end{aligned} \tag{35}$$

After substituting the above inequality into Eq. (34), the relation could be rewritten as:

$$\begin{aligned} J_i(t_{k+1}) &\le J_i^*(t_k) - \int_{t_k}^{t_{k+1}} L_i(x_i^*(\tau|t_k), u_i^*(\tau|t_k))d\tau \\ &\le J_i^*(t_k). \end{aligned} \tag{36}$$

Because of the inherent relation $J_i^*\left(t_{k+1}\right) \le J_i\left(t_{k+1}\right)$ in the optimization problem, $J_i^*\left(t_{k+1}\right) \le J_i^*\left(t_k\right)$ can be easily obtained. Therefore, the asymptotical local stability is proved by demonstrating the optimal cost is decreasing over time. □

Remark 3. The above proposition focuses on local stability. For the mathematical proof of the string stability, readers are referred to [17] and [33]. The reason why the string stability is not proved here is that additional coupled constraints are required in the aforementioned references. These extra coupled constraints for the string stability may result that the required conditions (18)-(20) for the feasibility and local stability are not satisfied under the derived sufficient conditions (22)-(24). The DMPC problem will be more complicated with additional coupled constraints, and the feasibility and stability are difficult to be guaranteed, which is the subject of further study. However, from the numerical experiments presented in the next section, it can be observed that in some scenarios, both local stability and string stability can be achieved. Yet, this conclusion for string stability has limitations in practical and complex scenarios, which will be shown in the simulation experiments in the next section.

IV. Simulation experiments and numerical analysis

To verify the effectiveness of the proposed DMPC approach and the derived stability conditions in realistic but complex scenarios, numerical experiments are carried out based on the data of the Beijing-Shanghai high-speed railway line. More specifically, the experiments contain three parts: i) the approach's control performance assessment given initial disturbances, e.g., initial speed differences or spacing errors; ii) control performance assessment considering external disturbances, e.g., varying maneuvers of the leading train due to varying speed limits; iii) a sensitivity analysis for the stable region of weight coefficients. The default values of simulation parameters are shown in Table III according to the data from practical high-speed trains and simulation settings in [23]. The proposed algorithm is conducted by the MATLAB R2018b on a PC (3.6-GHz Intel i7 CPU, 16-GB RAM, and 64-bit Windows 10). At each iteration step, the formulated optimal control problem is transcribed by YALMIP [34] and solved by the FMINCON function provided in the MATLAB optimization toolbox.

TABLE III
Simulation parameters

Parameters	Values	Units
m	490	t
N	4	-
$(D_L, D_{\min}, D_d)$	$(200, 50, 100)$	m
c_0	0.7550	N/kg
c_1	0.00636	N/(km/h·kg)
c_2	0.000115	N/(km^2/h^2 ·kg)
$(U_{\min}, U_{\max})$	$(-1, 1)$	m/s^2
(T_p, Tc)	$(5, 5)$	s
(p_1, p_2, q_1, q_2, R)	$(0.5, 0.5, 0.8, 0.4, 0.3)$	-
(k_s, k_v)	$(0, 0.1)$	-

TABLE IV
Average computational performance of centralized and distributed MPC for one time step

Algorithms	Number of trains	Iterations	CPU time (s)
Centralized MPC	4	140	1.78
	8	201	7.71
DMPC	4	31	0.21
	8	31	0.21

Under the given algorithm parameters, to illustrate the computational performance of the centralized MPC and the proposed DMPC algorithm clearly, the computational performance is listed in Table IV. Note that for the VCTS control problem, the controller needs to calculate output every time step; therefore, the CPU computation time shown here is an average value of all time steps under the operation scenario of case study 1 (Table V). It can be observed that the proposed DMPC algorithm is more efficient than the other. It is worth mentioning that the computation time will rise sharply when the number of trains increases; while for the DMPC, there is no such problem since each train only calculates its own sub-problem for the control task. It is understandable that the dimension and quantity of inputs for the DMPC controller are not increased with the expansion of the VCTS system. The optimal solution at each time step can be obtained within 1s, indicating that the proposed DMPC algorithm satisfies the real-time requirement and is more applicable in practical applications.

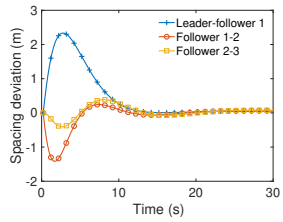

(a) Spacing deviation-time curve

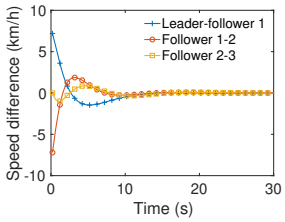

(b) Speed difference-time curve

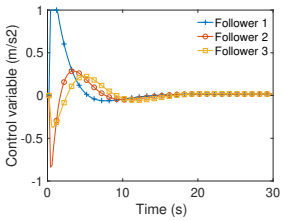

(c) Control variable-time curve

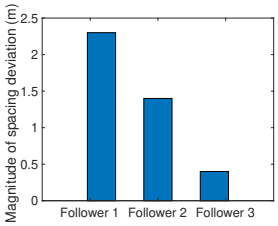

(d) Magnitude of spacing errors for each train

Fig. 4. Simulation results of case study 1 with initial speed difference.

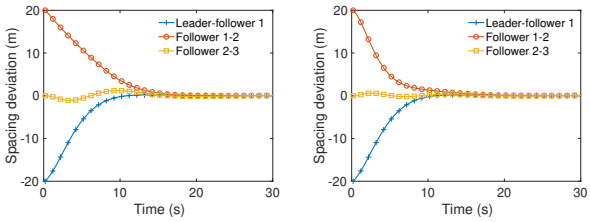

(a) Spacing deviation-time curve

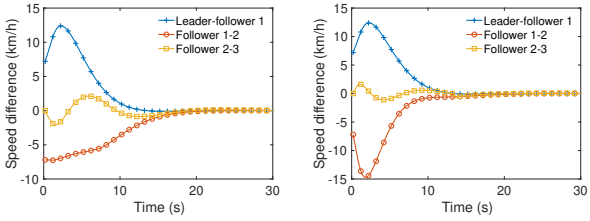

(b) Speed difference-time curve

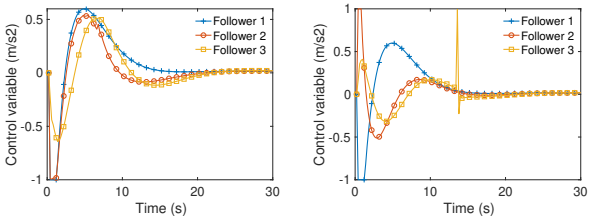

(c) Control variable-time curve

Fig. 5. Simulation results of case study 2 with initial speed differece and spacing error: left column is from the proposed approach and right column is from the alternative approach.

A. Experiment 1: control performance under initial disturbances

This experiment is conducted to inspect the control performance under initial disturbances. A VCTS contains four trains - one leading train and three following trains - cruising at 300km/h. The settings of the DMPC controller for each train are based on the sufficient conditions (22)-(24), as shown in Table III. The initial states (i.e., the number of considered trains in the VCTS, the spacing and velocity of each train, and the disturbance type) for the VCTS in these case studies are presented in Table V. For this experiment, the simulation time is 30s, and the running distance is about 2.5km.

In the first case study, there is an initial disturbance in the 1st following train whose speed is set as 292.8km/h, i.e., $[300, 292.8, 300, 300]$km/h for each train respectively, while the spacing errors are zero. The results in Fig. 4(a) and 4(b) show that the disturbance causes all following trains to deviate from the equilibrium state, and all deviations are eliminated at 15s. It can also be observed that maximum values of spacing errors of following trains decrease progressively in Fig. 4(d).

To better disclose the control performance and the safe operation, here we carry out a comparison between our approach and an approach that safety constraints of relative braking distance are only considered for terminal states [14]. This case study contains both the speed difference, i.e., 7.2km/h, and the spacing error, 20m, which are imposed on the 1st following train simultaneously. In detail, as shown in Fig. 5(a), the 1st following train needs to decelerate as the spacing between it and the leader is smaller than the desired 150m. This driving behavior of the 1st following train shows the same tendency in Fig. 5(c). However, for the 2nd and 3rd following trains, two approaches give different control sequences in Fig. 5(c), which leads to distinct speed profiles in Fig. 5(b). For instance, trains are slowed down in the proposed method while advanced in the other. The reason is that, due to the instant safety constraints for every predicted state explained in Eq. (12), the 2nd following train cannot speed up while the speed difference exists between it and the 1st following train. This illustration confirms that the proposed approach with instant safety constraints is effective and in line with the practical application.

Furthermore, in Fig. 5, the spacing error between the 2nd and the 3rd following trains is much smaller than that between the 1st and the 2nd ones, e.g., the magnitude of fluctuation is reduced into the range of $[-1.2, +1.4]$m. The above-mentioned results confirm the stability of the VCTS.

B. Experiment 2: control performance under external disturbances

This experiment is conducted to investigate the control performance under varying maneuvers of the leading train caused by external disturbances. The settings of the DMPC controller for each train are the same as Experiment 1 shown in Table III. The initial states (i.e., the number of considered trains in the VCTS, the spacing and velocity of each train, and the disturbance type) for the VCTS in this experiment are presented in Table VI.

In case study 3, four trains within a VCTS, including one leading train and three following trains, cruising at 300 km/h, are simulated. For better illustration, the initial disturbances are not included in this experiment; however, the control algorithm can handle mixed disturbances. The leading train has maximum traction and maximum braking during the cruising period. These varying maneuvers of the leading train lead to

TABLE V
INITIAL STATES OF EACH CASE STUDIES IN EXPERIMENT 1

Case study	VCTS composition	Initial spacing (m)	Initial speed (km/h)	Disturbance type
1	1 leader and 3 followers	[150,150,150]	[300,292.8,300,300]	Initial speed difference
2	1 leader and 3 followers	[130,170,150]	[300,292.8,300,300]	Initial speed difference and spacing error

TABLE VI
INITIAL STATES OF EACH CASE STUDIES IN EXPERIMENT 2

Case study	VCTS composition	Initial spacing (m)	Initial speed (km/h)	Disturbance type
3	1 leader and 3 followers	[150,150,150]	[300,300,300,300]	Maximum traction and braking
4	1 leader and 3 followers	[150,150,150]	[252,252,252,252]	Varying speed limits

TABLE VII
SPEED LIMITS OF THE SIMULATED LINE

Position (km)	Value of speed limits (km/h)
$0-7$	330
$7-11$	270
$11-16$	180
$16-20$	250

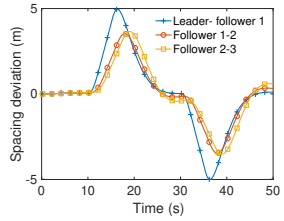

(a) Spacing deviation-time curve

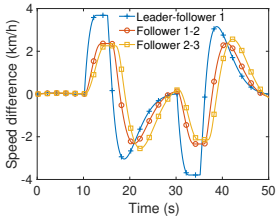

(b) Speed difference-time curve

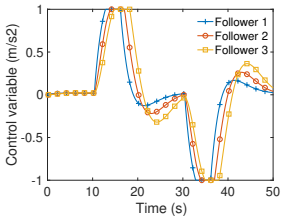

(c) Control variable-time curve

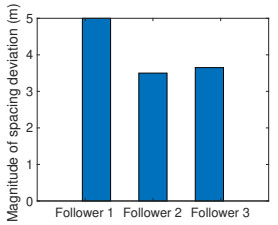

(d) Magnitude of spacing errors for each train

Fig. 6. Simulation results of case study 3 with maximum traction and braking maneuvers.

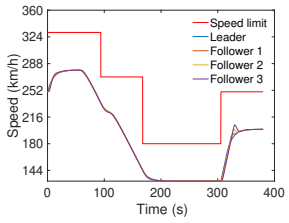

(a) Speed-time curve

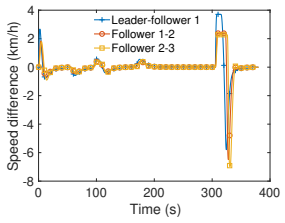

(b) Control variable-time curve

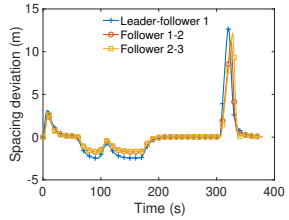

(c) Spacing deviation-time curve

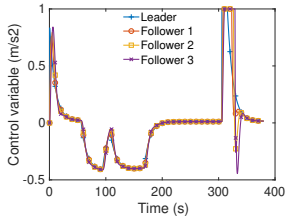

(d) Speed difference-time curve

Fig. 7. Simulation results of case study 4 with varying speed limits.

tracking errors in following trains with its predecessor, which may result in unstable fluctuation within the VCTS if without stability control. Results in Fig. 6 show that following trains can track varying maneuvers of the leading train effectively and converge to the equilibrium state gradually. In addition, the spacing errors caused by external disturbances are not attenuated along with the following trains in Fig. 6(d), i.e., $[5, 3.5, 3.65]$ for each following train respectively. These results reveal that the local stability is guaranteed but the string stability is not always ensured as mentioned in Remark 3.

Furthermore, speed limits are varying in the practical railway due to complex line conditions in the real world, which are the primary cause of frequently happened traction and braking during the cruising period. In the case study 4, actual speed limits are taken into account and the simulated distance is extended to 20km to include a wide range of speed limits, which are shown in Table VII. In Fig. 7, it can be observed that the proposed control method can cope with the continuously changing speed limits, guaranteeing the stability of the VCTS. Spacing deviations and speed differences increase gradually right after the speed limit jumps and decrease over time if trains enter the cruising stage. All the errors shown in Fig. 7(c) and 7(d) are within a certain small range, e.g., $[-2.5, 12.5]$m for spacing deviations and $[-6.9, 3.7]$km/h for speed differences, respectively. However, due to the suddenly changed speed limits as shown in Fig. 7(c), the spacing between trains has significant variations and the string stability is not indicated in this case as the spacing error between the 2nd and the 3rd following trains is slightly larger than that between the 1st and the 2nd ones.

C. Experiment 3: a sensitivity analysis for the stable region of weight coefficients

In this experiment, we further examine the influence of different parameter settings on the stability conditions and the stable region for parameters. The exact stable region for weight coefficients in Eq. (14)-(16), (p_1, p_2, q_1, q_2, R),

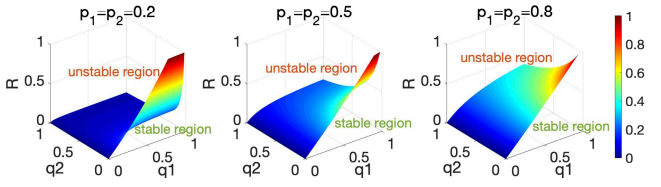

Fig. 8. Illustration of stable region.

are analyzed and presented in this section, considering the sufficient conditions (22)-(24) according to Proposition 1.

The main motivation of this experiment is that these coefficients are associated with distinct control performance. In detail, if $q_1 > q_2$, the controller is more focused on reducing spacing errors; otherwise, mitigating speed differences are more stressed. A larger value of R means the current train's controller cares more about tracking the control variable of its preceding train. However, we cannot just emphasize the performance indicators but ignore the feasibility and stability of the controller. p_1 and p_2 represent the weight of terminal costs, which play an important role in the guarantee of stability. By setting different values of weight coefficients, Fig. 8 shows the stable region of (q_1, q_2, R) for the DMPC controller under various (p_1, p_2). The unstable and stable regions are above and below the color surface, respectively, according to the sufficient conditions (22)-(24). This implies that weight coefficients should be selected within the stable region to guarantee stability. Furthermore, the stable region is directly affected by the values of (p_1, p_2), as shown in Fig. 8. This result ties in closely with the "three ingredients" referred in [27], i.e., terminal cost (p_1, p_2), terminal constraint set $\mathcal{X}_f$ and terminal controller π^f, which are found useful in developing stable MPC controllers. We can also observe that the stable condition is stricter in the case of $p_1 = p_2 = 0.2$ than that of others, as the color surface is lower. This implies that, in this VCTS control problem, slightly larger weight coefficients p_1 and p_2 can help improve the stability and give more options to other coefficients to gain different control performance.

V. Conclusion

This paper proposed a DMPC method for the high-speed VCTS control with guaranteed feasibility and stability. An optimal control formulation is constructed in the DMPC framework considering the coupled constraint of safety braking distance and the individual constraints of speed limit variations and restricted traction/braking performance. For rigor, this study designed the terminal invariant set and the terminal controller for the DMPC algorithm and provided mathematical proofs for the feasibility and stability of the DMPC controller. Numerical experiments were conducted to verify the proposed control algorithm and the propositions and more importantly, to illustrate the feasibility and stability for a VCTS running on a section of a high-speed railway line under varying speed limits and disturbances. The proposed DMPC algorithm also showed efficiency in solving the VCTS control problem, especially when the VCTS system is expanded with more trains, which satisfies the real-time requirement and is more applicable in practical applications. In addition, the stable region for coefficients was derived from the stability conditions, and different case studies were tested to prove the correctness of the mathematical proofs. The results show that coefficients of controller selected within the stable region can guarantee the asymptotic stability under initial and external disturbances.

In future studies, we will address more on uncertain air-drag disturbances caused by strong wind and tunnels when trains are operating at high speed, as these uncertainties would directly affect the stable operation of a high-speed VCTS. In addition, the feasibility and stability analysis of the DMPC controller for a VCTS will be more critical and challenged with uncertain disturbances and coupled constraints.

Acknowledgment

The authors would like to thank Chen Peng from University of Leeds for inspiring discussions and useful comments.

References

[1] C. Cheron, M. Walter, J. Sandor, and E. Wiebe, "ERRAC roadmap. towards 2030: Energy, noise and vibration european railway roadmaps," *Procedia - Social and Behavioral Sciences*, vol. 48, pp. 2221–2229, 2012.

[2] Y. Wang, B. De Schutter, T. J. van den Boom, and B. Ning, "Optimal trajectory planning for trains under fixed and moving signaling systems using mixed integer linear programming," *Control Engineering Practice*, vol. 22, pp. 44–56, 2014.

[3] E. Quaglietta, M. Wang, and R. Goverde, "A multi-state train-following model for the analysis of virtual coupling railway operations," in *Proceedings of the 8th International Conference on Railway Operations Modelling and Analysis*, 2019, pp. 1382–1401.

[4] M. Haltuf, "Shift2Rail JU from member state's point of view," *Transportation Research Procedia*, vol. 14, pp. 1819–1828, 2016.

[5] L. Liu, P. Wang, W. Wei, Q. Li, and B. Zhang, "Intelligent dispatching and coordinated control method at railway stations for virtually coupled train sets," in *2019 IEEE Intelligent Transportation Systems Conference (ITSC)*, 2019, pp. 607–612.

[6] I. Mitchell, E. Goddard, F. Montes, P. Stanley, R. Muttram, W. Coenraad, J. Poré, S. Andrews, and L. Lochman, "ERTMS level 4, train convoys or virtual coupling," *IRSE NEWS*, vol. 219, pp. 1–3, 2016.

[7] R. Liu, A. Whiteing, and A. Koh, "Challenging established rules for train control through a fault tolerance approach: applications at a classic railway junction," *Proceedings of the Institution of Mechanical Engineers, Part F: Journal of Rail and Rapid Transit*, vol. 227, no. 6, pp. 685–692, 2013.

[8] R. Liu, "Simulation model of speed control for the moving-block systems under ERTMS level 3," in *2016 IEEE International Conference on Intelligent Rail Transportation (ICIRT)*, 2016, pp. 322–327.

[9] J. Chen, R. Liu, D. Ngoduy, and Z. Shi, "A new multi-anticipative car-following model with consideration of the desired following distance," *Nonlinear Dynamics*, vol. 85, no. 4, pp. 2705–2717, 2016.

[10] C. Di Meo, M. Di Vaio, F. Flammini, R. Nardone, S. Santini, and V. Vittorini, "ERTMS/ETCS virtual coupling: Proof of concept and numerical analysis," *IEEE Transactions on Intelligent Transportation Systems*, pp. 1–12, 2019.

[11] V. Turri, B. Besselink, and K. H. Johansson, "Cooperative look-ahead control for fuel-efficient and safe heavy-duty vehicle platooning," *IEEE Transactions on Control Systems Technology*, vol. 25, no. 1, pp. 12–28, 2016.

[12] Z. Yao, L. Shen, R. Liu, Y. Jiang, and X. Yang, "A dynamic predictive traffic signal control framework in a cross-sectional vehicle infrastructure integration environment," *IEEE Transactions on Intelligent Transportation Systems*, vol. 21, no. 4, pp. 1455–1466, April 2020.

[13] W. Zhao, D. Ngoduy, S. Shepherd, R. Liu, and M. Papageorgiou, "A platoon based cooperative eco-driving model for mixed automated and human-driven vehicles at a signalised intersection," *Transportation Research Part C: Emerging Technologies*, vol. 95, pp. 802–821, 2018.

[14] J. Felez, Y. Kim, and F. Borrelli, "A model predictive control approach for virtual coupling in railways," *IEEE Transactions on Intelligent Transportation Systems*, vol. 20, no. 7, pp. 2728–2739, 2019.

[15] M. Wang, W. Daamen, S. P. Hoogendoorn, and B. van Arem, "Rolling horizon control framework for driver assistance systems. Part I: Mathematical formulation and non-cooperative systems," *Transportation Research Part C: Emerging Technologies*, vol. 40, pp. 271–289, 2014.

[16] Y. Zhou, S. Ahn, M. Chitturi, and D. A. Noyce, "Rolling horizon stochastic optimal control strategy for ACC and CACC under uncertainty," *Transportation Research Part C: Emerging Technologies*, vol. 83, pp. 61–76, 2017.

[17] Y. Zhou, M. Wang, and S. Ahn, "Distributed model predictive control approach for cooperative car-following with guaranteed local and string stability," *Transportation Research Part B: Methodological*, vol. 128, pp. 69–86, 2019.

[18] Y. Zhou and S. Ahn, "Robust local and string stability for a decentralized car following control strategy for connected automated vehicles," *Transportation Research Part B: Methodological*, vol. 125, pp. 175–196, 2019.

[19] L. Dai, Q. Cao, Y. Xia, and Y. Gao, "Distributed MPC for formation of multi-agent systems with collision avoidance and obstacle avoidance," *Journal of the Franklin Institute*, vol. 354, no. 4, pp. 2068–2085, 2017.

[20] S. Gao, H. Dong, B. Ning, and Q. Zhang, "Cooperative prescribed performance tracking control for multiple high-speed trains in moving block signaling system," *IEEE Transactions on Intelligent Transportation Systems*, vol. 20, no. 7, pp. 2740–2749, 2019.

[21] S. Li, L. Yang, and Z. Gao, "Distributed optimal control for multiple high-speed train movement: An alternating direction method of multipliers," *Automatica*, vol. 112, p. 108646, 2020.

[22] W. Bai, Z. Lin, H. Dong, and B. Ning, "Distributed cooperative cruise control of multiple high-speed trains under a state-dependent information transmission topology," *IEEE Transactions on Intelligent Transportation Systems*, vol. 20, no. 7, pp. 2750–2763, 2019.

[23] J. Xun, J. Yin, R. Liu, F. Liu, Y. Zhou, and T. Tang, "Cooperative control of high-speed trains for headway regulation: A self-triggered model predictive control based approach," *Transportation Research Part C: Emerging Technologies*, vol. 102, pp. 106–120, 2019.

[24] Q. Wu, M. Spiryagin, and C. Cole, "Longitudinal train dynamics: an overview," *Vehicle System Dynamics*, vol. 54, no. 12, pp. 1688–1714, 2016.

[25] H. Ye and R. Liu, "A multiphase optimal control method for multi-train control and scheduling on railway lines," *Transportation Research Part B: Methodological*, vol. 93, pp. 377–393, 2016.

[26] S. Feng, Y. Zhang, S. E. Li, Z. Cao, H. X. Liu, and L. Li, "String stability for vehicular platoon control: Definitions and analysis methods," *Annual Reviews in Control*, vol. 47, pp. 81–97, 2019.

[27] D. Mayne, J. Rawlings, C. Rao, and P. Scokaert, "Constrained model predictive control: Stability and optimality," *Automatica*, vol. 36, no. 6, pp. 789–814, 2000.

[28] P. D. Christofides, R. Scattolini, D. Muñoz de la Peña, and J. Liu, "Distributed model predictive control: A tutorial review and future research directions," *Computers and Chemical Engineering*, vol. 51, pp. 21–41, 2013.

[29] F. Borrelli, P. Falcone, T. Keviczky, J. Asgari, and D. H. , "MPC-based approach to active steering for autonomous vehicle systems," *International Journal of Vehicle Autonomous Systems*, vol. 3, no. 2-4, pp. 265–291, 2005.

[30] P. Falcone, F. Borrelli, J. Asgari, H. E. Tseng, and D. Hrovat, "A model predictive control approach for combined braking and steering in autonomous vehicles," in *2007 Mediterranean Conference on Control Automation*, June 2007, pp. 1–6.

[31] Z. Sun, L. Dai, K. Liu, Y. Xia, and K. H. Johansson, "Robust MPC for tracking constrained unicycle robots with additive disturbances," *Automatica*, vol. 90, pp. 172–184, 2018.

[32] D. Swaroop and J. K. Hedrick, "String stability of interconnected systems," *IEEE Transactions on Automatic Control*, vol. 41, no. 3, pp. 349–357, 1996.

[33] S. Feng, H. Sun, Y. Zhang, J. Zheng, H. X. Liu, and L. Li, "Tube-based discrete controller design for vehicle platoons subject to disturbances and saturation constraints," *IEEE Transactions on Control Systems Technology*, vol. 28, no. 3, pp. 1066–1073, 2020.

[34] J. Löfberg, "YALMIP: A toolbox for modeling and optimization in MATLAB," in *2004 IEEE International Conference on Robotics and Automation*, Taipei, Taiwan, 2004, pp. 284–289.

Yafei Liu received the B.S. degree from Beijing Jiaotong University, Beijing, China, in 2016, where he is currently pursuing the Ph.D. degree with the State Key Laboratory of Rail Traffic Control and Safety. His current research interests include intelligent operation and optimal control in railway systems.

Ronghui Liu received the B.S. degree from Peking University, China, and the Ph.D. degree from Cambridge University, U.K. She is currently a Professor with the Institute for Transport Studies, University of Leeds, U.K. Her main research interest lies in developing traffic micro-simulation models to analyze the dynamic and complex travel behavior and interactions in transport networks.

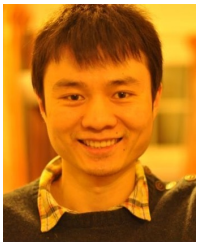

Weichong Feng received the B.Sc. degree in computational and applied mathematics and the M.Sc. degree in vehicle engineering from Southwest Jiaotong University, Chendu, China, in 2009 and 2011, respectively, and the Ph.D. degree in mechanical engineering from the University of Birmingham, Birmingham, U.K., in 2015. After two and a half years Postdoctoral research period, he joined the School of Mechanical Engineering, Shanghai Jiao Tong University as an Assistant Professor (tenure-track). He moved to the Institute of Transport Studies, University of Leeds as a Research Fellow in 2018. He is currently a Lecturer with the School of Mechanical and Aerospace Engineering, Queen's University Belfast, Belfast, UK. His current research interests include decision making and control of intelligent vehicles, human-centric autonomous driving, cooperative automation, and dynamics and control of mechanical systems.

Jing Xun received the Ph.D. degree from Beijing Jiaotong University, Beijing, China, in 2012. He is currently an Associate Professor with the State Key Laboratory of Rail Traffic Control and Safety, Beijing Jiaotong University. His current research interests include advanced train control methods, optimization problem in rail transport, traffic flow theory, cellular automata, and reinforcement learning.

Tao Tang received the Ph.D. degree in engineering from the Chinese Academy of Sciences, Beijing, China, in 1991. He is currently a Professor with the School of Electronics and Information Engineering and the Director of the Rail Traffic Control and Safety State Key Laboratory, Beijing Jiaotong University, Beijing, China. His research interests include communication-based train control, high-speed train control, and intelligent transportation systems.